NANO LETTERS

xxxx
Vol. 0, No. 0
A−D

Ballistic Transport in Metallic Nanotubes with Reliable Pd Ohmic Contacts

David Mann, Ali Javey, Jing Kong,† Qian Wang, and Hongjie Dai*

Department of Chemistry and Laboratory for Advanced Materials, Stanford University, Stanford, California 94305

Received August 25, 2003; Revised Manuscript Received September 23, 2003

ABSTRACT

Contacting metallic single-walled carbon nanotubes by palladium (Pd) affords highly reproducible ohmic contacts and allows for the detailed elucidation of ballistic transport in metallic nanotubes. The Pd ohmic contacts are more reliable than the titanium (Ti) previously used for ballistic nanotube devices. In contrast, Pt contacts appear to give nonohmic contacts to metallic nanotubes. For both ohmic and nonohmic contacts, the length of the nanotube under the metal contact area is electrically turned off. Transport occurs from metal to nanotube at the edges of the contacts. Measurements with large numbers of Pd-contacted nanotube samples reveal that the mean free path for defect scattering in SWNTs grown by chemical vapor deposition can be up to 4 μm. The mean free paths for acoustic phonon scattering are on the order of 500 nm at room temperature and $\gg$4 μm at low temperatures.

Ohmic contacts with minimum contact resistance are important to the fundamental characterization and realization of high-performance devices of electronic materials. Ohmic contacts to individual metallic single-walled carbon nanotubes (m-SWNTs) by Cr and Ti have enabled the observation of ballistic electron transport in SWNTs.[1,2] The hallmark of ballistic transport in SWNTs with ideal contacts is conductance approaching the quantum limit of $G = 4e^2/h$ (resistance $R \approx 6.5$ kΩ) and the manifestation of phase-coherent resonance transport at low temperatures.[1,2] More recently, ohmic contacts to semiconducting SWNTs (s-SWNTs) have been achieved with Pd electrodes.[3] The high work function of Pd and its favorable interactions with nanotube sidewalls afford largely suppressed Schottky barriers at the Pd/s−SWNT contacts, allowing for the observation of ballistic transport through the valence band of s-SWNTs. The on-states of ohmically contacted semiconducting SWNTs exhibit similar characteristics to ballistic metallic tubes with $G \approx 4e^2/h$ and current delivery capability, reaching the optical phonon scattering limit of $\sim$25 μA per tube.[3]

In this letter, we report highly reliable ohmic contacts to metallic SWNTs made by Pd. Compared to other metals such as Ti, Pd is unique in giving ohmic contacts to m-SWNTs with very high reproducibility. In addition to two terminal m-SWNTs with ohmic contacts, devices with a segment of the metallic tube covered by Pd or Pt are fabricated and investigated by transport measurements. Furthermore, the ohmically contacted m-SWNT devices allow for the elucidation of electron transport properties that are intrinsic to the nanotube material. Several important parameters for m-SWNTs grown by chemical vapor deposition (CVD) are estimated, including the mean free paths (mfp) for scattering by defects or imperfections and by acoustic phonons.

Individual metallic SWNT devices were fabricated by the patterned CVD growth[4] of SWNTs on SiO_2/Si wafers, followed by electron beam lithography (EBL), metal deposition, and liftoff to form source/drain (S/D) top contacts.[5] The heavily doped Si substrate was used as a back gate, and the thickness of the SiO_2 gate dielectric was either 500 or 67 nm. The thickness of the S/D metal (Pd or Ti) electrodes was $\sim$30 nm deposited by electron beam evaporation in a $<10^{-7}$ Torr vacuum. Devices with Pd S/D contacts were annealed at 220 °C in Ar for 10 min. In most cases, Pd ohmic contacts to m-SWNTs were found to form without the annealing step.

We first present results obtained with metallic SWNTs contacted by Ti at the S/D. Previously, we have reported ballistic transport in ohmically contacted relatively short (L$\sim$200 nm) m-SWNTs with Ti S/D electrodes.[2] Since then, we have observed ballistic transport in CVD-grown metallic tubes with lengths up to 4 μm. Figure 1a shows an ultrastraight nanotube (diameter $d \approx 1.7$ nm) with a length of 4 μm between Ti S/D contacts. The conductance of the device (measured under V_{ds}=1 mV) exhibits little gate dependence, as expected for metallic tubes, and monotonically increases from $\sim e^2/h$ ($R \approx 32$ kΩ) to $\sim 3e^2/h$ ($R \approx 8.6$ kΩ) as the sample is cooled from 290 to 4 K. Between 4 K and 300 mK in a ^{3}He cryostat, pronounced slow conductance oscillations versus the gate voltage (V_g) are

* Corresponding author. E-mail: hdai@stanford.edu.
† Current address: Department of NanoScience and DIMES, Delft University of Technology, Lorentzweg 1, 2628 CJ Delft, The Netherlands.

10.1021/nl034700o CCC: $25.00
Published on Web 00/00/0000

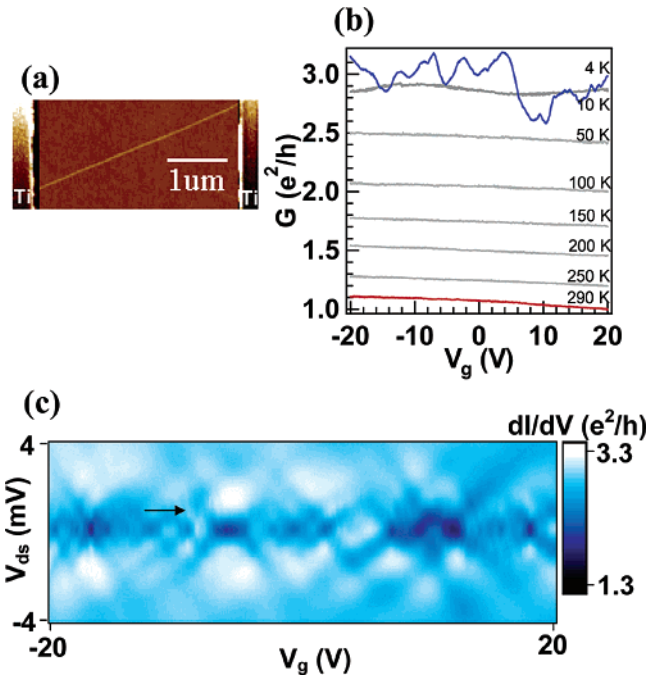

Figure 1. (a) Atomic force microscopy (AFM) image of a 4-μm-long SWNT ($d \approx 1.7$ nm) contacted by Ti at S/D. (b) Conductance (G) vs V_g curves recorded at various temperatures from 290 to 4 K. (c) Differential conductance (dI/dV_{ds}) vs V_g and V_{ds} recorded at 300 mK. The arrow points to the characteristic conductance peak at $V_c \approx 0.75$mV for the 4-μm-long tube.

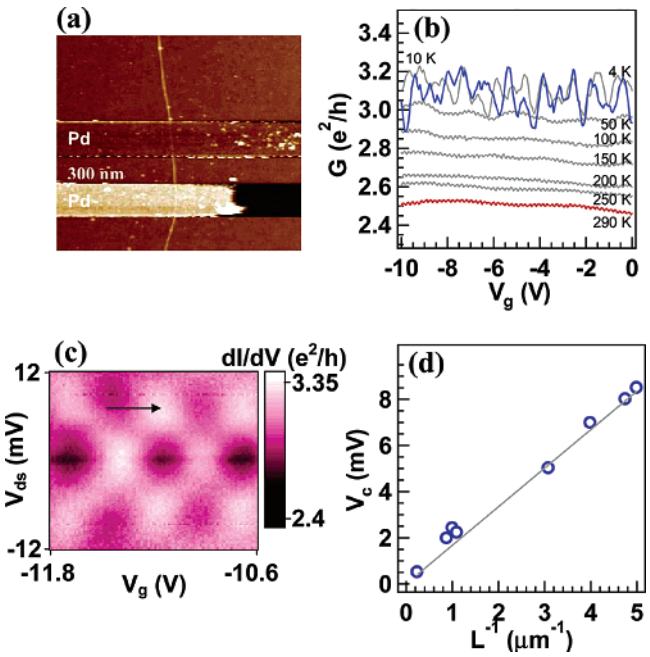

Figure 2. (a) AFM image of a 300-nm SWNT ($d \approx 3$ nm) contacted by Pd electrodes. (b) G vs V_g curves from 290 to 4 K. (c) dI/dV_{ds} vs V_g and V_{ds} recorded at 1.5 K showing clear conductance oscillations with $V_c = 7$ mV (shown by an arrow). (d) Plot of V_c vs the inverse tube length L. The slope of the line is $h\upsilon_F/2e = 1.670$ mV·μm where $\upsilon_F = 8.1 \times 10^5$m/s. The data points are from a few representative Pd-contacted devices.

observed, and differential conductance dI/dV_{ds} versus V_g and V_{ds} exhibits an interference pattern with conductance peaks and valleys at $V_{ds} = 0$ (Figure 1c). The results strongly point to a nearly ideal Ti/m-SWNT sample with highly transparent contacts (transmission probability at the two contacts $t_{Ti,1} \approx t_{Ti,2} \approx 0.85$ and $G \approx t_{Ti,1} \times t_{Ti,2} \times 4e^2/h \approx 3e^2/h$). There are no significant defects along the 4-μm length of the nanotube because no conductance degradation due to weak localization[2,6] is observed down to 300 mK. The somewhat irregular interference pattern does point to a nonideal Fabry−Perot resonator.[1] This irregularity is attributed to minor disorder or inhomogeneity along the full length of the tube. A 3-fold conductance increase from 290 to 4 K is observed and attributed to the quenching of acoustic phonon (AP) scattering.[2,3,6,7] Thus, for this particular device, one can glean that the mfp for defect scattering in the SWNT is $l_d > 4$ μm, and that the mfp's for acoustic phonon scattering are $l_{AP}(290K) < 4$ μm and $l_{AP}(300\ mK) > 4$ μm.

The nearly ideal long ballistic SWNT sample with Ti contacts shown above is admittedly rare. It is also found that ohmic contacts to m-SWNTs by Ti have a limited success rate of ∼10−20%. Relatively large fluctuations in contact resistance (10−100 kΩ) exist in different batches of devices. The ballistic mfp of 4 μm is observed once out of dozens of 3−4-μm-long m-SWNTs.

In contrast to Ti, Pd affords ohmic contacts to metallic tubes with high reproducibility. Nearly all of the Pd contacted metallic SWNTs with lengths $L \leq 1$ μm exhibit conductance on the order of $2e^2/h$ ($R \approx 10-20$ kΩ) at 290 K and approach $4e^2/h$ at 4K (Figure 2b for $L = 300$ nm, Figure 3c and Figure 4c for $L = 1$ μm). At low temperatures, the devices exhibit clear interference patterns in dI/dV_{ds} versus V_g and V_{ds} (Figure 2c). The interference patterns for various-length SWNTs are consistent with the Fabry−Perot resonators described by Liang et al.[1] Whenever the phase shift acquired by electrons during a round trip in a SWNT reaches $2L \times eV_{ds}/\hbar_F = 2\pi$ where $\upsilon_F = 8.1 \times 10^5$m/s is the Fermi velocity, a resonance peak occurs at $V_{ds} = V_c = \pi\hbar_F/eL$. Plotting V_c versus $^1/_L$ gives a line with a slope[1] of $h\upsilon_F/2e = 1.670$ mV·μm, which is the case in our Pd-contacted m-SWNT samples (Figure 2d).

The mfp for defect scattering is a parameter specific to each individual SWNT and can be up to $l_d \approx 4$ μm (Figure 1). On the basis of measurements of tens of Pd/m-SWNT devices, we conclude that the average mfp for defect scattering is $l_d \approx 1$ μm for our CVD-grown nanotubes. For most devices with longer tube lengths, conductance versus temperature data tend to show a downturn at low temperatures, signaling weak localization effects due to imperfections in the tube. It is also found that smaller-diameter SWNTs (<1.5 nm) are more likely to have various degrees of bends along the tube length. These tubes tend to become more insulating at low temperatures and have shorter l_d values due to imperfections related to mechanical deformation.

We observe that the conductance of shorter m-SWNTs exhibits weaker temperature dependence than longer ones. The $L = 4$-μm-long m-SWNT exhibits a 3-fold conductance increase (from e^2/h to $3e^2/h$) from 290 to 4 K (Figure 1b). However, the $L \approx 300$ nm tubes typically exhibit a 30% conductance increase (from $2.5e^2/h$ to $3.2e^2/h$) upon cooling.

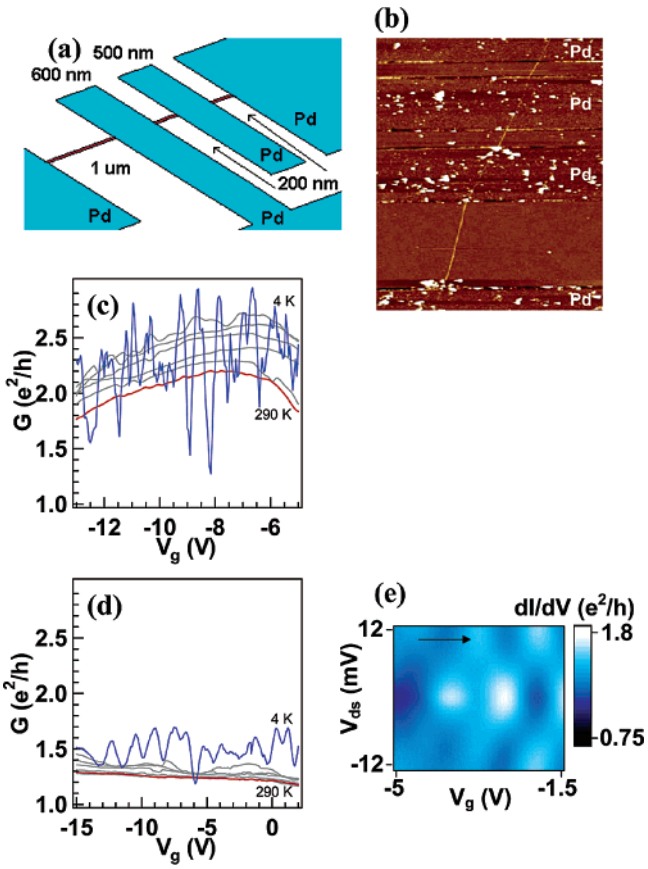

Figure 3. (a) Schematic drawing of two types of devices formed on a single SWNT. The first type consists of an ~1-μm-long SWNT between two Pd S/D electrodes. The second type is similar except for a Pd strip covering part of the SWNT between two Pd electrodes. All of the metal structures were formed by one step of EBL, Pd metal deposition, and a liftoff process. (b) AFM image of the SWNT ($d \approx 3$ nm) structures depicted in a. (c) G vs V_g recorded from 290 to 4 K for the SWNT without Pd coverage between S/D. (d) G vs V_g recorded from 290 to 4 K for the device with additional Pd coating in the middle. (e) dI/dV_{ds} vs V_g and V_{ds} at 1.5 K. Conductance peaks at $V_c = 8.5$ mV (at the arrow) correspond to tube resonators ~200 nm in length (similar to the lengths of the tube sections free of Pd coating).

The resistance in m-SWNTs due to acoustic phonon scattering can be written as

$$R_{AP}(T) = \left(\frac{h}{4e^2}\right)\left[\frac{L}{l_{AP}(T)}\right]$$

Fitting of the measured resistance of long and short SWNTs to this expression (the physical meaning of which is that resistance due to acoustic phonon scattering scales with tube length L and is negligible if $l_{AP} \ll L$) provides a rough estimate of $l_{AP}(290\ \text{K}) \approx 500$ nm for acoustic phonon scattering at room temperature.

In Figure 3c, we show that a 1-μm-long Pd-contacted m-SWNT exhibits ballistic transport with conductance up to ~$3e^2/h$ at 4 K. On the same tube, a similar device is fabricated except for a Pd stripe covering a ~500-nm-long segment of the tube between the Pd S/D (Figure 3a and b). Electrical measurements reveal that the conductance of the

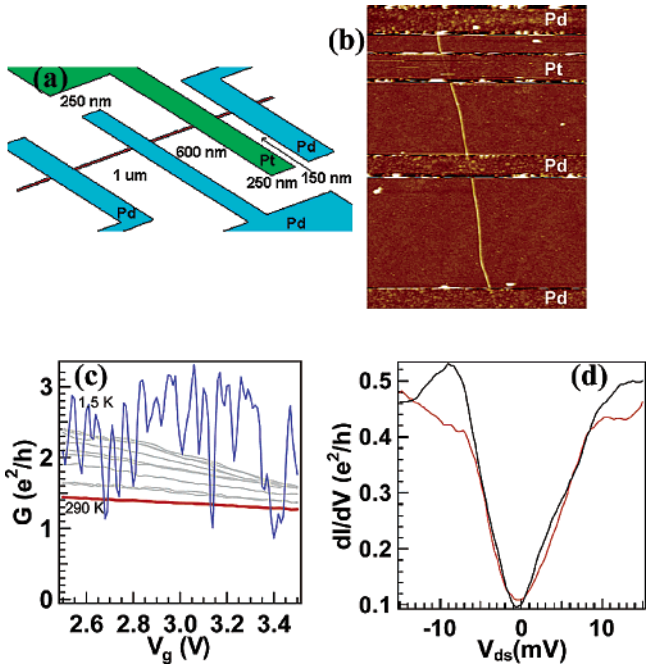

Figure 4. (a) Schematic drawing of two types of devices formed on a single SWNT. The first type consists of an ~1-μm-long SWNT between two Pd S/D electrodes. The second type is similar except for a Pt electrode placed onto the SWNT between two Pd electrodes. The Pt electrode was formed by a second step of EBL, Pt deposition (by sputtering), and liftoff after the first step for Pd. The offset of the Pt electrode from the center was due to misalignment. (b) AFM image of the SWNT structure ($d \approx 3.2$ nm) depicted in a. (c) G vs V_g curves recorded from 290 to 1.5 K for a SWNT between two Pd S/D contacts. The small, rapid conductance oscillations from 290−50 K are attributed to noise in the measurement system. (d) dI/dV vs V_{ds} measured at 1.5 K (under two gate voltages) for the SWNT between two Pd contacts with an additional Pt electrode placed in between. The dip structure exists over the entire V_g range scanned.

partially Pd-covered SWNT is limited below $2e^2/h$ (Figure 3d; the uncovered device is limited below $4e^2/h$), and the interference pattern exhibits a characteristic energy scale ($V_c \approx 8.5$ mV along the bias axis, Figure 3e) approximately corresponding to SWNT resonators with a tube length of $L \approx 200$ nm that matches the lengths of the two uncoated tube segments. This suggests that the Pd stripe has divided the nanotube into two Fabry−Perot resonators in series. It is clear that the electron transmission probability at the four Pd−SWNT contact junctions is near unity ($t_{pd} \approx 0.9$) and that the nanotube segment covered by Pd is electrically turned off. This result illustrates the high reproducibility of Pd ohmic contacts to m-SWNTs. It also shows that electron transport into (or out of) an m-SWNT from (or into) a Pd top contact occurs at the edge of the Pd electrode.

Different results are obtained with an m-SWNT partially covered with Pt along its length between Pd S/D (Figure 4a and b). At 290 K, the conductance measured between Pd S/D is 3 times lower ($G \approx 0.4e^2/h$; $R \approx 65$ kΩ; data not shown) than that of the same tube without Pt coverage (Figure 4c, $G \approx 1.5e^2/h$; $R \approx 17$ kΩ). Multi-probe measurements (with the Pt strip as an electrode) reveal that the resistance between the Pd S/D equals the sum of the

resistance measured between S(Pd)−Pt and Pt−Pd(D). These results lead to the conclusion that, first, the Pt−SWNT contact is nonohmic (nonohmic contacts have been reported by Dekker et al. previously[8,9]) and has a resistance of ∼20 kΩ. Second, despite the relatively low transmission probability at Pt−SWNT contacts, electrons mostly transmit in and out of the Pt strip with the Pt-covered section turned off. At 1.5 K, the SWNT without a Pt coating exhibits a high conductance of $\sim 3.3e^2/h$ and interference effect (Figure 4c). In strong contrast, the Pt-coated device is more insulating below ∼50 K, with a clear conductance dip in dI/dV_{ds} versus V_{ds} at $V_{ds} = 0$ (Figure 4d). The pronounced conductance dips (for some V_g) appear to be consistent with the known effect of the Coulomb blockade in single-tunnel junction[10,11] devices (the Pt-covered sample can be considered to be two back-to-back Pd−SWNT−Pt systems, each with an ohmic contact and a tunnel junction). Detailed results and an analysis of this phenomenon will be presented elsewhere.

We have shown here that Pd gives highly reliable and reproducible ohmic contacts to metallic SWNTs, a result that is not surprising considering ohmic contacts made to semiconducting nanotubes by Pd.[3] Ti ohmic contacts to m-SWNT are less reliable despite excellent wetting of SWNT sidewalls by Ti.[12,13] This could be due to the high chemical reactivity of Ti toward oxidation, and the quality of the contact is sensitive to metal deposition conditions such as vacuum. Pt contacts are nonohmic to both metallic and semiconducting SWNTs. The chemical nature of the Pd−SWNT and Pt−SWNT interfaces must be responsible for the differences in electrical transmission and remains elusive at the present time. In the metal-on-top contact configuration for both ohmic and nonohmic contacts, the bulk length of the tube under the metal appears to be electrically off, and transport occurs from metal to nanotube at the edges of the contact. This is consistent with the insensitivity of contact resistance to the contact length for SWNTs. With large numbers of ohmically contacted m-SWNT samples, we find that the mean free path for defect scattering in our CVD-grown material is typically 1 μm and can be up to 4 μm. The mean free paths for acoustic phonon scattering are on the order of 500 nm at room temperature and >4 μm below 4 K.

Acknowledgment. This work was supported by ABB Group Ltd., MARCO MSD Focus Center, DARPA/Moletronics, a Packard Fellowship, a Sloan Fellowship, and a Dreyfus Teacher-Scholar award.

References

(1) Liang, W.; Bockrath, M.; Bozovic, D.; Hafner, J.; Tinkham, M.; Park, H. *Nature* **2001**, *411*, 665−669.
(2) Kong, J.; Yenilmez, E.; Tombler, T. W.; Kim, W.; Liu, L.; Jayanthi, C. S.; Wu, S. Y.; Laughlin, R. B.; Dai, H. *Phys. Rev. Lett.* **2001**, *87*, 106801.
(3) Javey, A.; Guo, J.; Wang, Q.; Lundstrom, M.; Dai, H. J. *Nature* **2003**, *424*, 654−657.
(4) Kong, J.; Soh, H.; Cassell, A.; Quate, C. F.; Dai, H. *Nature* **1998**, *395*, 878.
(5) Soh, H.; Quate, C.; Morpurgo, A.; Marcus, C.; Kong, J.; Dai, H. *Appl. Phys. Lett.* **1999**, *75*, 627−629.
(6) Fischer, J. E.; Dai, H.; Thess, A.; Lee, R.; Hanjani, N. M.; Dehaas, D. L.; Smalley, R. E. *Phys. Rev. B* **1997**, *55*, R4921−R4924.
(7) Kane, C. L.; Mele, E. J.; Lee, R.; Fischer, J. E.; Petit, P.; Dai, H.; Thess, A.; Smalley, R. E.; Verschueren, A. R. M.; Tans, S. J.; Dekker, C. *Eur. Phys. Lett.* **1998**, *6*, 683−688.
(8) Tans, S.; Devoret, M.; Groeneveld, R.; Dekker, C. *Nature* **1998**, *394*, 761−764.
(9) Yao, Z.; Kane, C. L.; Dekker, C. *Phys. Rev. Lett.* **2000**, *84*, 2941−2944.
(10) Grabert, H.; Devoret, M. H., Eds. *Single Charge Tunneling*; Plenum: New York, 1992.
(11) Wahlgren, P.; Delsing, P.; Claeson, T.; Haviland, D. B. *Phys. Rev. B* **1998**, *57*, 2375−2381, and references therein.
(12) Zhang, Y.; Franklin, N.; Chen, R.; Dai, H. *Chem. Phys. Lett.* **2000**, *331*, 35−41.
(13) Zhang, Y.; Dai, H. *Appl. Phys. Lett.* **2000**, *77*, 3015−3017.

NL034700O